



UNIVERSIDAD DE CUENCA

Facultad de Ingeniería

Maestría en Hidrología con mención en Ecohidrología

Characterization of the stable isotopic composition of precipitation, surface, and subsurface waters in a small Andean catchment in northern Ecuador.

Trabajo de titulación previo a la obtención del título de Magíster en Hidrología con mención en Ecohidrología

Autor:

Braulio César Lahuate Imbaquingo

CI: 092356662-4

Correo electrónico: [brauliolahuate@gmail.com](mailto:brauliolahuate@gmail.com)

Director:

Giovanny Mauricio Mosquera Rojas Ph.D.

CI: 010445091-1

**Cuenca - Ecuador**

15-diciembre-2021



## Resumen:

La combinación de datos hidrométricos tradicionales con trazadores ambientales como los isótopos estables en el agua ha demostrado ser valiosa para mejorar la comprensión hidrológica de las cuencas. Sin embargo, la aplicación de trazadores isotópicos en las cabeceras de los Andes tropicales sigue siendo limitada. La composición isotópica de la precipitación, el agua del suelo a lo largo de dos laderas experimentales con diferente cobertura vegetal (pajonal y almohadillas), los humedales y el caudal recolectados cada dos semanas durante un año se utilizaron para mejorar la comprensión de la hidrología de una cuenca de páramo del norte de Ecuador. El análisis de la composición isotópica de la precipitación indica que, aunque la precipitación local se forma en condiciones de equilibrio isotópico, está influenciada por procesos de reciclaje de humedad. Con respecto al comportamiento hidrológico, la variabilidad espacio-temporal de las señales isotópicas y el análisis de los proxies de tiempo de tránsito inverso (ITTP) de las aguas superficiales (descarga) y subsuperficiales (agua del suelo y humedales) sugieren que las rutas de flujo vertical son dominantes a través de la cuenca. Las composiciones isotópicas fuertemente amortiguadas de estas aguas sugieren además una alta capacidad de almacenamiento de agua en la cuenca, lo que aumenta el tiempo de tránsito o la edad del agua en el sistema hidrológico. Las señales isotópicas y los ITTP también muestran la importancia de los reservorios de agua subterránea bien mezclados en la hidrología del sistema. El conocimiento hidrológico desarrollado en este estudio no solo aumenta la comprensión de la generación y regulación de caudal en los páramos del norte de Ecuador, sino que también se puede utilizar para mejorar la gestión de los recursos hídricos en la región dado que permite focalizar acciones de intervención en territorio evaluando si dichas intervenciones podrían tener impacto sobre los componentes que controlan la hidrología de la cuenca.

**Palabras claves:** Isotopos estables. Deuterio. Oxígeno 18. Exceso de deuterio. ITTP. Andes. Trópicos. Precipitación. Suelos. Humedales. Caudal. Antisana.



**Abstract:**

Combining traditional hydrometric data with environmental tracers such as water stable isotopes has proven valuable to improve the understanding of catchment hydrology. Nevertheless, the application of isotopic tracers in headwater catchments of the tropical Andes remains limited. The stable isotopic composition of precipitation, soil water along two experimental hillslopes with different vegetation cover (tussock grass and cushion plants), wetlands, and discharge collected biweekly during one year was used to improve the understanding of the hydrology of a northern Ecuadorian paramo catchment. The analysis of the stable isotopic composition of precipitation indicates that although local precipitation forms under isotopic equilibrium conditions, it is influenced by moisture recycling processes. Regarding catchment hydrological behavior, the spatio-temporal variability of isotopic signals and the analysis of inverse transit time proxies (ITTPs) of surface (discharge) and subsurface (soil water and wetlands) waters suggest that vertical flow paths are dominant across the catchment. Strongly damped isotopic compositions of these waters further suggest a high water storage capacity of the catchment, increasing the transit time or age of water in the hydrological system. Isotopic signals and ITTPs also show the importance of well-mixed subsurface water reservoirs in the hydrology of the system. The hydrological knowledge developed in this study not only increases the understanding of discharge generation and regulation in northern Ecuadorian Paramos, but also can be used to improve the management of water resources in the region. Field restoration activities could be focused on trying to improve the catchment's components that control its hydrology.

**Keywords:** Water stable isotopes. Deuterium. D-excess. ITTP. Andes. Tropics. Precipitation. Soils. Wetlands. Discharge. Antisana.



## **Acknowledgment**

I would like to thank all the people who made this work possible. First of all, to my whole family who have always been there for me. We were through a lot during these years. To my director and supervisor team for all the academic support along this journey. To my job, FONAG, for conceding to me the opportunity to make a pause in my activities to develop myself in a professional, and academic way.

My sincerely gratefulness to the ParamoSus project for funding my Master. ParamoSus is a collaboration effort between Ecuadorian and Belgian academic institutions, EPMAPS-Q and FONAG. The project provided not only the funding for the Master's program, but also designed and installed the experimental setup that was used during this thesis, took the water samples, and covered support's expenses during the program. Special thanks to Sebastian Paez for helping with sample collection within the study area while I was in Cuenca. Without this help nothing of this could have been possible. To my supervisor team regarding isotopes: Giovanni Mosquera, Patricio Crespo, and Xavier Zapata. Thanks for all the teachings. I found this topic really interesting, and I hope to work in the future with you developing new knowledge.

Finally, to the University of Cuenca, specially to iDRHICA department, for providing all the infrastructure, laboratories, and staff necessary to study this Master.



## Índice del Trabajo

1. Introduction	7
2. Materials and Methods	8
3. Results	14
4. Discussion	20
5. Conclusions	24
6. Appendix A	24
7. References	25



## Índice de Figuras

Figure 1. Study Area and experimental setup.	11
Figure 2. Time series of precipitation amount and $\delta^{18}\text{O}$ . $\delta^{18}\text{O}$ - $\delta^2\text{H}$ relation in local precipitation (LMWL).	15
Figure 3. $\delta^{18}\text{O}$ - $\delta^2\text{H}$ relation in soil water, wetlands (WE) at the bottom of each hillslope, and discharge at the catchment outlet (Q).	16
Figure 4. Spatio-temporal variation of the biweekly isotopic composition of precipitation and soil water.	18
Figure 5. Spatio-temporal variation of the biweekly isotopic composition of precipitation, wetlands at the bottom of the cushion plant (CU) and tussock grass (TU) experimental hillslopes, and discharge at the catchment outlet (Q).	18
Figure 6. Inverse Transit Time Proxies (ITTPs) of soil water.	20



## Índice de Tablas

Table 1. Location of tussock grass and cushion plants pits, and soil profile characterization at each pit. Soil horizon depth refers to the soil horizon depth within the soil profile. CU: cushion plants experimental hillslope. TU: Tussock grass experimental hillslope. UPR, UP, MI. and LO correspond to upper replica, upper, middle, and lower sampling position respectively. 10

Table 2. Depth of installed soil-water samplers (suction cups or SC, and wick samplers or WS) along the experimental hillslopes. CU: cushion plants experimental hillslope. TU: Tussock grass experimental hillslope. UPR, UP, MI. and LO correspond to upper replica, upper, middle, and lower sampling position respectively. 12

Table 3. Summary statistics of the isotopic composition ( $\delta^{18}\text{O}$  and d-excess=  $\delta^2\text{H}-8\delta^{18}\text{O}$ ) and inverse transit time proxies (ITTPs) in soil water collected using suction cups (SC) and wick samplers (WS) at the upper (UP), upper replica (UPR), middle (MI), and lower (LO) parts of the cushion plant (CP) and tussock grass (TU) experimental hillslopes, wetlands at the bottom of the cushion plant (CP) and tussock grass (TU) experimental hillslopes, discharge at the catchment outlet (Q), and precipitation (P) during the period March 2019-March 2020. Sampling depths for each soil water sampler are shown in Table 2. n=number of samples. 16



## Cláusula de licencia y autorización para publicación en el Repositorio Institucional

---

Yo, Braulio César Lahuatte Imbaquingo en calidad de autor y titular de los derechos morales y patrimoniales del trabajo de titulación "Characterization of the stable isotopic composition of precipitation, surface, and subsurface waters in a small Andean catchment in northern Ecuador", de conformidad con el Art. 114 del CÓDIGO ORGÁNICO DE LA ECONOMÍA SOCIAL DE LOS CONOCIMIENTOS, CREATIVIDAD E INNOVACIÓN reconozco a favor de la Universidad de Cuenca una licencia gratuita, intransferible y no exclusiva para el uso no comercial de la obra, con fines estrictamente académicos.

Asimismo, autorizo a la Universidad de Cuenca para que realice la publicación de este trabajo de titulación en el repositorio institucional, de conformidad a lo dispuesto en el Art. 144 de la Ley Orgánica de Educación Superior.

Cuenca, 15 de diciembre de 2021

---

Braulio César Lahuatte Imbaquingo

0923566624





## Cláusula de Propiedad Intelectual

---

Yo, Braulio César Lahuate Imbaquingo, autor del trabajo de titulación “Characterization of the stable isotopic composition of precipitation, surface, and subsurface waters in a small Andean catchment in northern Ecuador”, certifico que todas las ideas, opiniones y contenidos expuestos en la presente investigación son de exclusiva responsabilidad de su autor.

Cuenca, 15 de diciembre de 2021

---

Braulio César Lahuate Imbaquingo

0923566624



## 1. Introduction

Headwater catchments in the tropical Andes provide many ecosystem services including erosion control, carbon sequestration, nutrient cycling, food provisioning, and production of high-quality water (Aparecido et al., 2017; Wright et al., 2017). The latter is favored by the continuous input of rainfall throughout the year (Celleri et al., 2007) in combination with the unique properties of soils such as high-water retention, regulation, and infiltration capacities (Buytaert et al., 2005), which allow for an uninterrupted supply of water. This resource is crucial to support the development of major cities in the region such as Mérida, Bogotá, Cuenca, and Quito (Buytaert & Bièvre, 2012). These cities satisfy their hydroelectric, irrigation, domestic, and industrial needs by using water originated in headwater catchments (Céleri & Feyen, 2009).

Despite the importance of these catchments, there are still some regions within the tropical Andes where hydrology is not thoroughly understood. In particular, the catchment-scale hydrological knowledge in the northern Ecuadorian Andes remains scarce. Through the sole use of traditional hydrometric measurements, Ochoa-Tocachi et al., (2016) analyzed the hydrological dynamics and gave important insights into the variable water yield of some headwater catchments in the region highlighting the importance of better understanding subsurface water dynamics. Even though the complementary use of environmental tracers such as water stable isotopes or geochemical data has proven valuable to obtain process-based understanding of catchment hydrological behavior (Inamdar et al., 2013; Mosquera et al., 2020), the use of these tracers in the northern Andes of Ecuador has been limited to high frequency studies in catchments fed mainly by glaciers melting and hillslopes runoff (Minaya et al., 2016). The use of a larger data set of water stable isotopes has not been yet applied within the northern Ecuadorian Andes.

Water stable isotopes are natural tracers that have been useful in catchment hydrology, given the diversity of analyses that are derived from them (Kendall & McDonnell, 1998; Leibundgut et al., 2009). The determination of the local meteoric water line (LMWL, i.e., the regression between the stable isotopes of hydrogen,  $\delta^2\text{H}$ , and oxygen,  $\delta^{18}\text{O}$  in local precipitation) has been used to establish precipitation moisture sources entering tropical Andean catchments during different seasons (Esquivel-Hernández et al., 2019; Windhorst et al., 2013). The LMWL slope and intercept (D-excess) also show if evaporation plays a major role in the hydrology of surface water bodies (Brooks et al., 2012). Characterization of the isotopic composition of precipitation, surface, and subsurface waters in tropical regions has been used to delineate water flow paths within catchments (Crespo et al., 2011; Minaya et al., 2016; Mosquera, Céleri, et al., 2016; Muñoz-Villers et al., 2016),



quantify catchment passive storage (Lazo et al., 2019), and develop conceptual catchment hydrological models (Mosquera et al., 2020). Water stable isotopes are essential to improve the understanding of catchment hydrology, however, their application is still limited in tropical regions, and the Andean region is no exception. This issue is due to the scarcity of isotopic monitoring networks (Mosquera, Céleri, et al., 2016). Although isotopic studies in the tropical Andes have been predominantly carried out in the south of Ecuador where old volcanism produced shallow soils and compact bedrock is found close to the surface (Molina et al., 2019), it is not usually applied to environments with recent volcanic activity during the Holocene that provided input of volcanic ash and produced deeper soils where bedrock is deeper buried (Hall et al., 2017). The limited tracer studies in the northern Ecuadorian Andes limit the improvement of catchment hydrological knowledge and therefore the efficacy of water management-related institutions that work in these highlands. Improving hydrological knowledge could help these institutions to better direct the efforts and resources that they spend within the field.

Limited hydrological knowledge is a hindrance to adequate catchment management strategies (Pataki et al., 2011). Therefore, adequate management needs to respond not only to science but also to society's needs (Falkenmark & Folke, 2002). In this context, institutions pursuing to manage Andean headwater catchments in a socio-hydrological way have emerged. Those institutions, however, often lack scientific-based knowledge over which to rely on management and conservation efforts. A thorough understanding of catchment hydrology across different time and spatial scales is key to support water management institutions and their interest in guaranteeing water availability to future generations. In this sense, water stable isotopic studies can help increase hydrological knowledge that can be used for decision-making by determining catchment storage and different flow paths that water follows up to the streams.

Private and public institutions are making great efforts to manage headwater catchments along the Andes. Specifically, in the northern Ecuadorian Andes, those institutions are buying and instrumenting headwater catchments to study their hydrology (EPMAPS & FONAG, 2018). Important insights have been acquired in terms of determining runoff coefficients. However, there is still a lack of knowledge about catchment hydrological behavior. This study addresses this issue by using water stable isotopes to answer the following research questions in a northern Ecuadorian catchment from which Quito obtains part of its potable water.

- What are the spatio-temporal patterns of the isotopic composition of precipitation, soil-water, wetlands, and discharge in a small headwater catchment in north Ecuador?



- How does water mix at the catchment scale?

## 2. Materials and Methods

### 2.1 Study Area

This research was developed in a small headwater catchment situated within the Jatunhuaycu Experimental Observatory (JEO, 0°30'19"S, 78°14'29"W; Fig. 1a,b). The observatory covers an area of 32.6 km<sup>2</sup> of Paramo ecosystem and used to be part of a cattle farm until 2011 (EPMAPS & FONAG, 2018). The observatory is located in the northern Ecuadorian Andes, specifically within the Antisana Water Conservation Area which is 55 km southeast of Quito city. At the moment, Quito's Water Fund (FONAG), and Empresa Pública Metropolitana de Agua Potable y Saneamiento (EPMAPS-Q) own the observatory and are actively researching its hydrology, ecology, and the impacts of conservation efforts since 2011 in collaboration with academic partner institutions. FONAG manages the study catchment given that it feeds Mica's reservoir, an important water source for EPMAPS-Q and Quito inhabitants (EPMAPS & FONAG, 2018). This study was carried out in micro-catchment 1 (0.66 km<sup>2</sup>), hereafter referred as JTU\_01 (Fig. 1c). JTU was equipped in the scope of the ParamoSUS project, a joint collaboration effort between Ecuadorian and Belgian academic institutions, EPMAPS-Q and FONAG.

JTU\_01 has a mean annual precipitation of 641 mm and a mean annual discharge of 59 mm, presenting a very low runoff coefficient (annual discharge to precipitation) of 0.09 (Ochoa-Tocachi et al., 2016). Regarding the catchment's soils, those near Antisana Volcano are deep, reaching depths around 5 to 7 m since they are a sequence of buried soils due to active volcanoes in the area. In other areas closed to La Mica Lagoon, buried soils have been observed beneath scoria and glacial-fluvial sediments up to 27 meters in depth. The soils are young and slightly altered vitric andosols (Calispa et al., 2021; Onderet, 2018). Histosols are common in flat zones where organic matter is accumulated (EPMAPS & FONAG, 2018). Both types of soils have high water regulation and retention capacity, low bulk density, and high saturated hydraulic conductivity (Páez-Bimos et al., 2020). The land use in JEO was grazing until 2011, and now is 100 % conservation. The vegetation is distributed as follows: tussock grass 48%, cushion plants 40 %, and others 12% (EPMAPS & FONAG, 2018). Regarding geology, in the study area, we found the Pisayambo geological formation which is characterized by a lithology of Andesitic lava and ashfall deposit.

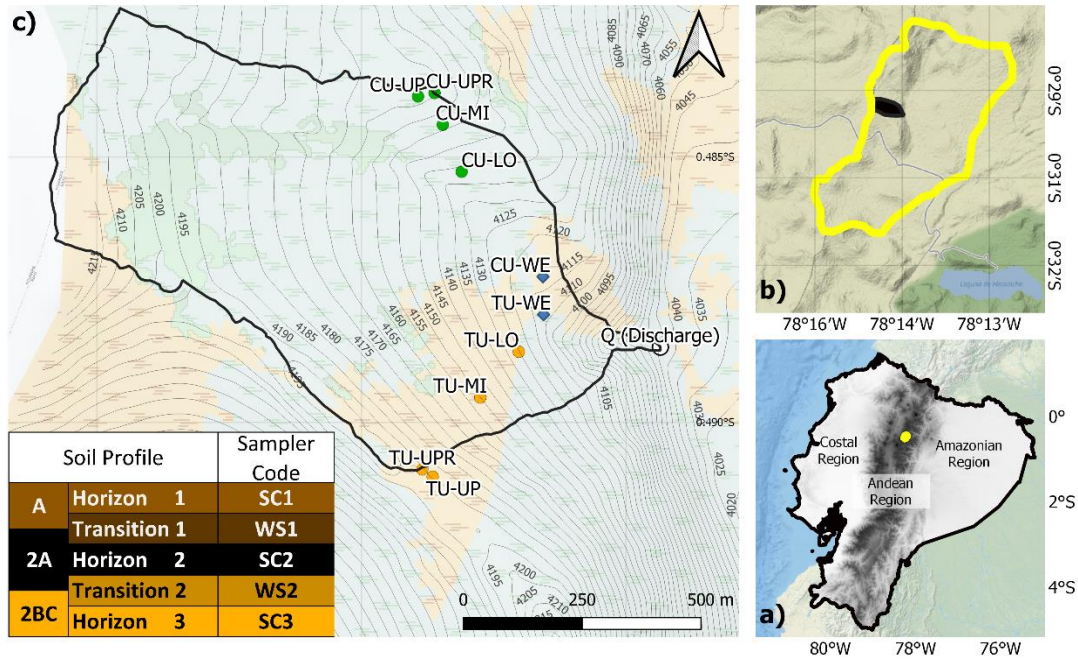


Figure 1. a) Location of the Jatunhuaycu Experimental Observatory (JEO) in the northern Ecuadorian Andes. b) Microcatchment 1 (JTU\_01) within the JEO. c) Monitoring setup of ParamoSUS project (Vanacker et al., 2017) at JTU\_01 including the Tussock grass (TU, orange circles) and Cushion plant (CU, green circles) experimental hillslopes showing the location of the soil water samplers at the upper (UP), upper replica (UPR), middle (MI), and lower (LO) parts of the hillslope, the wetlands (WE) at the bottom of each hillslope (blue circles), and discharge station (white circle). Subplot c) also shows an example of a representative soil profile (horizons A, 2A, 2BC) within the catchment (Calispa et al., 2021). Suction cups (SC) were used to collect soil water at the A, 2A, and 2BC horizons and wick samplers (WS) were used to collect soil water at the interface of the A-2A and 2A-2BC horizons. At the CU\_UP position a rain gauge and a precipitation water sampler were installed.

## 2.2 Experimental Design

To better understand hydrological behavior, two experimental hillslopes at JTU\_01 were implemented and monitored as part of the ARES PRD ParamoSUS project (Vanacker et al., 2017). Each one consisted of four sampling positions, upper (UP), upper replica (UPR), middle (MI), and lower (LO). At the end of both hillslopes, wells were installed. These wells consisted of 2 inches diameter by 2 meters long PVC pipes that were placed vertically within the wetland. Holes were drilled along the pipe to allow soil-water to recharge the well. A v-notch gauge was also monitored at the catchment outlet. All sampling sites along the hillslopes were implemented with soil-water samplers. A precipitation water sampler and a rain gauge were installed at the upper part of the cushion hillslope. The experimental setup in JTU\_01 is presented in Fig. 1c. The monitored hillslopes differed in dominant vegetation cover. One was dominated by tussock grasses (*Calamagrostis intermedia*) and the other by cushion plants (*Azorella pedunculata*). Hereafter, we will refer to them as TU and CU, respectively. At each sampling position in both hillslopes, the soils were characterized up to a depth of 135 cm following the (FAO, 2015) guidelines. Five soil



horizons were determined, namely O, A, 2A, 2BC, 3BC, but only the A, 2A, 2BC were monitored (Calispa et al., 2021). Their depth at each sampling location along the experimental hillslopes is presented in Table 1. It is important to mention that despite the tussock well is installed within the wetland, its location immediately below the tussock slope (contour lines in Fig. 1c) means that it is a transition between the hillslope and the wetland.

*Table 1. Location of tussock grass and cushion plants pits, and soil profile characterization at each pit (Calispa et al., 2021). Soil horizon depth refers to the soil horizon depth within the soil profile. CU: cushion plants experimental hillslope. TU: Tussock grass experimental hillslope. UP, UPR, MI, and LO correspond to upper, upper replica, middle, and lower sampling position, respectively.*

Position	Coordinates	Altitude (m.a.s.l.)	Soil Horizon depth (cm)				
			O	A	2A	2BC	3BC
TU_UR	0°29'27.6" S / 78°14'38.4" W	4191	0-5	5-30	30-70	70-85	85-110
TU_UPR	0°29'27.6" S / 78°14'38.4" W	4183	0-5	5-30	30-70	70-85	85-110
TU_MI	0°29'24" S / 78°14'34.8" W	4156	0-4	4-27	27-70	70-95	95-115
TU_LO	0°29'20.4" S / 78°14'31.2" W	4132	0-7	7-45	45-92	92-110	110-135
CU_UPR	0°29'2.4" S / 78°14'38.4" W	4165	0-8	8-30	30-60	60-80	80-102
CU_UP	0°29'2.4" S / 78°14'38.4" W	4166	0-8	8-30	30-60	60-80	80-102
CU_MI	0°29'2.4" S / 78°14'34.8" W	4157	0-8	8-32	32-70	70-103	103-125
CU_LO	0°29'6" S / 78°14'34.8" W	4138	0-10	10-40	40-75	75-110	110-120

Within the ParamoSUS project, the team collected biweekly samples of water in precipitation, soil, wetlands, and discharge during the period March 2019 to March 2020 (Páez-Bimos et al., 2020). Precipitation samples were collected using a polypropylene collector covered with aluminum foil. A 5 mm thick oil layer was added into the collector to prevent isotopic fractionation due to evaporation (Mook, 2000). The team collected soil-water samples using two types of samplers, specifically, ceramic suction cups (SC) and fiber glass wick samplers (WS). SCs were used in the A, 2A, and 2BC horizons (Fig. 1c and Table 2). SCs are lysimeters that consist of three parts: the suction cup itself, the sampling bottle, and the suction container. The SCs were 0.50 m in length and had a ceramic cup with a maximum pore size of 1  $\mu$ m at one end. During each sampling campaign, a negative pressure between 45 to 50 KPa was applied to the SCs to collect water from the soil into a 500 ml glass bottle. A hose was connected to the glass bottles, covered with aluminum foil, and placed inside closed buckets. To collect water in the transition horizons (A-2A, and 2A-2BC), the team used wick samplers. Wick samplers consist of 30 by 30 cm polypropylene plates in which 9.5 mm-diameter fiberglass wicks were untangled. The wicks were placed in direct contact with the soil by digging a hole within the soil pit at the depth of interest. To ensure that all the plate was in contact with the soil matrix a press was used to tighten the sampler in the dug hole. A 2-inch PVC tube connected the bottom of the plates with a 1-gallon plastic container. A suction of 55



cm was applied to the wicks (Singh et al., 2018). The codification of soil-water samplers was established by Vanacker et al., (2017) and includes information about the hillslope dominant vegetation cover (TU or CU), sampling position (UP, UPR, MI, or LO), soil water sampling device (SC or WS), and soil horizon or transition (1 for shallow, 2 for intermediate, and 3 for deep). For example, TU\_UP\_SC1 corresponds to the suction cup (SC) placed in the tussock slope (TU), upper position (UP), and in the A horizon (First Horizon) (Table 2 and Fig. 1c). Accordingly, CU\_LO\_WS1 corresponds to the wick sampler placed in the cushion slope, lower position, and between the transition of A to 2A horizons (First transition, Table 2 and Fig. 1c). Finally, wetlands and discharge were sampled directly from the wells and in-stream.

Table 2. Depth of installed soil-water samplers (suction cups or SC, and wick samplers or WS) along the experimental hillslopes (Vanacker et al., 2017). CU: cushion plants experimental hillslope. TU: Tussock grass experimental hillslope. UP, UPR, MI, and LO correspond to upper, upper replica, middle, and lower sampling position, respectively.

Position	Samplers' depth (cm)				
	A <sup>1</sup>	A-2A <sup>1</sup>	2A <sup>1</sup>	2A-2BC <sup>1</sup>	2BC <sup>1</sup>
	SC1 <sup>2</sup>	WS1 <sup>2</sup>	SC2 <sup>2</sup>	WS2 <sup>2</sup>	SC3 <sup>2</sup>
TU_UPR	17.5	30	50	70	77.5
TU_UP	17.5	30	50	70	77.5
TU_MI	15.5	27	48.5	70	82.5
TU_LO	26	45	68.5	92	101
CU_UPR	19	30	45	60	70
CU_UP	19	30	45	60	70
CU_MI	20	32	51	70	86.5
CU_LO	20.5	40	57.5	75	92.5

Note:

<sup>1</sup> Corresponding soil horizon or transition in which the sampler was installed (from left to right represents the soil profile).

<sup>2</sup> Samplers' code,

### 2.3 Water Stable Isotopes Laboratory Analysis

Immediately after collecting the water from all the sampling sites during the bi-weekly monitoring campaigns, they were filtered using a 0.45 µm pore RC membrane, and 2 ml amber glass bottles were filled with the filtered water. Then, the samples were transported and stored without being exposed to light to prevent isotopic fractionation due to evaporation (Mook, 2000). The samples were analyzed in the University of Cuenca's soil and water chemical analysis laboratory. Water stable isotopes ( $\delta^2\text{H}$  or Deuterium, and  $\delta^{18}\text{O}$ ) were determined using a Picarro L2130-i isotope water vapor analyzer that has a precision of 0.5 ‰ for  $\delta^2\text{H}$  and 0.1 ‰ for  $\delta^{18}\text{O}$ . Three secondary standards were used to calibrate the Picarro instrument and ensure analysis quality. To reduce the memory effect, the samples were analyzed by batches containing similar water sample types, and during each analysis, six injections were done into the analyzer and the first three were discarded. The measurements of the last three injections were compared to the equipment precisions and the secondary standards' standard deviations. If the measurements



were above the precisions the analysis was repeated. ChemCorrect 1.2.0 software was used to verify if contamination occurred. Only one soil sample was contaminated representing 0.08 % of all the samples. The results are presented in  $\delta$  notation using the Vienna Standard Mean Ocean Water (V-SMOW) as reference (Craig, 1961).

## 2.4 Isotopic spatio-temporal variation and mixing analysis

To assess isotopic spatio-temporal variation in precipitation, we plotted the isotopic composition together with the precipitation amount. We described how the isotopic composition varied based on the precipitation amount along the study period. Moreover, we calculated the linear correlation between  $\delta^2\text{H}$  and  $\delta^{18}\text{O}$  in precipitation to determine the local meteoric water line LMWL. The LMWL was used as quality control for the mixing analysis of soils, wetlands, and discharge since we verified that all the samples lay close to the LMWL and corresponded to a mixture of precipitation within the catchment. Soils, wetlands, and discharge isotopic composition were plotted and compared to precipitation composition to assess their spatio-temporal variation. We described the influence that precipitation input composition had over the different sampling positions and depths by visually analyzing if the response was directly related or showed a contrary behavior.

A second-order isotopic parameter, “D-excess”, was calculated for all the collected samples using the following equation:  $\text{D-excess} = \delta^2\text{H} - 8\delta^{18}\text{O}$  (Dansgaard, 1964). D-excess values in precipitation were used as a proxy for determining vapor source regions by comparing our D-excess values to the 10‰ value obtained in the global meteoric water line GMWL (Craig, 1961). Also, the D-excess values in soils, wetlands, and discharge were compared to precipitation D-excess since lower D-excess values mean that samples suffered post rainfall evaporation (Kendall & Coplen, 2001). We calculated the following metrics for the isotopic composition and D-excess: the number of samples, maximum and minimum value, standard deviation, and mean.

Concerning mixing processes, it is assumed that precipitation input composition is conserved as it travels through the system (Jasper et al., 2015; Kim & Jung, 2014). The subsurface movement of the water through internal catchment flow paths causes attenuation of the precipitation input signal due to advection and dispersion processes. When the tracer arrives to a sampling position (soil samplers, wells, or discharge), it has been affected by these processes and therefore its signal reflects the subsurface hydrological dynamics occurring within the catchment (Hrachowitz et al., 2016; Kirchner, 2016; McGuire & McDonnell, 2006). The inverse transit time proxies ITTPs (Tetzlaff et al., 2009) were used to identify differences in internal flow paths of water through the catchment. ITTP is a simple metric of tracer signal





damping, which is the ratio between the standard deviation of  $\delta^{18}\text{O}$  in an outflow to the standard deviation of  $\delta^{18}\text{O}$  in precipitation. To determine the standard deviation for the outflows and the precipitation we used all the samples collected during the study period for each collector. The lower the ITTP, the greater the attenuation and the transit time. Tetzlaff et al., (2009) found that ITTPs of 0.5 to 0.6 corresponded to mean transit times of around 4 months. ITTPs of 0.2 to 0.3 corresponded to mean transit times of 6 to 12 months. ITTPs lower than 0.1 corresponded to mean transit times of 1 to 3.5 years.

### 3. Results

#### 3.1 Precipitation isotopic composition

Precipitation amount and precipitation isotopic composition are presented in Fig. 2. The precipitation regime during the study period was bimodal with two precipitation peaks (Fig. 2a). The first rainy season started in March 2019 and finalized in June 2019 when a dry season started. This dry season lasted until late September 2019. The next wet season took place from then up to March 2020, but during this wet period two dry biweeks were registered (late January and late February 2020; Fig. 2a). The precipitation isotopic composition followed closely the temporal dynamic of precipitation amount. That is, depleted isotopic values ( $< -15\text{‰}$  in  $\delta^{18}\text{O}$ ) were observed during the wettest periods (e.g., Mar-Jun 2019 and Oct 2019-Jan 2020), and enriched isotopic values ( $> -10\text{‰}$  in  $\delta^{18}\text{O}$ ) were found during the driest periods (e.g., Jun-Sep 2019 and Feb 2020). Figure 2b shows that the  $\delta^{18}\text{O}$ - $\delta^2\text{H}$  relation in local precipitation (i.e., LMWL) had a similar slope (8.2) if compared to the GMWL (8), indicating that evaporation does not affect the isotopic composition of local precipitation (Kendall & McDonnell, 1998). Therefore, the results hereafter shown for mixing processes will be focused on  $\delta^{18}\text{O}$  as it reflects the temporal dynamics of both water stable isotopes. The intercept (D-excess) of the LMWL was higher (16.15‰) than that of the GMWL (10‰), indicating the effect of reevaporated moisture sources in local precipitation.

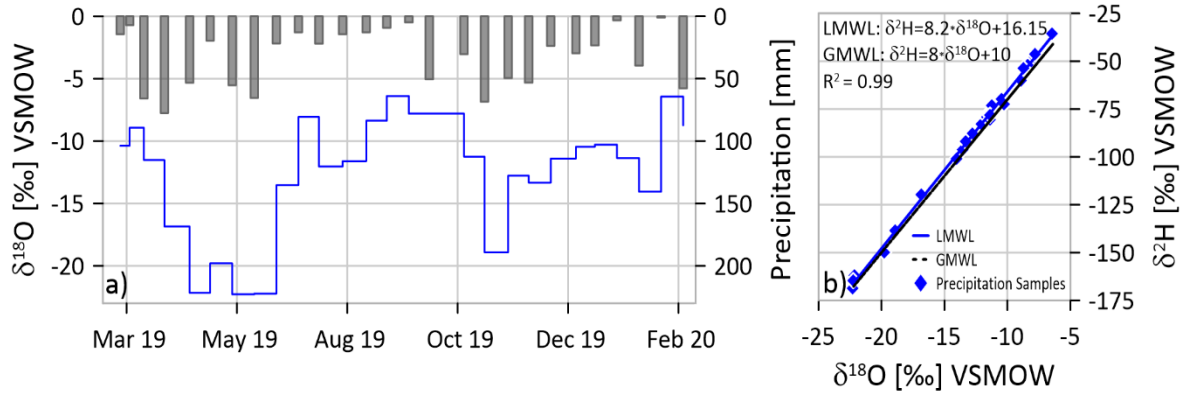


Figure 2. a) Biweekly time series of precipitation amount (grey bars) and  $\delta^{18}\text{O}$  isotopic composition (blue line). b)  $\delta^{18}\text{O}$ - $\delta^2\text{H}$  relation in local precipitation showing the local meteoric water line (LMWL) and the global meteoric water line (GMWL).

### 3.2 Soils, Wetlands, and Discharge Isotopic Composition

The isotopic composition of soil water, wetlands, and discharge is presented in Fig. 3. It is observed that all the collected samples lie within or very close to the LMWL. These observations depict that they are composed of a mixture of precipitation from different rainfall events. The TU\_UPR\_SC1 and TU\_UPR\_WS1 sampling sites registered the most depleted isotopic compositions (Fig. 3g). With regard to enriched values, none of the samples had concentrations higher than  $-10.6$  ‰ in  $\delta^{18}\text{O}$  and  $-77$  ‰ in  $\delta^2\text{H}$  (Fig. 3 and Table 3). A slight shift (D-excess) is observed in soil water under cushions plants, wetlands, and discharge in relation to the LMWL. Those samples consistently plotted below the LMWL, while soil water under tussock grass lied closer to it, with mean D-excess values for soils under cushion plants were lower than those in the soils underlying tussock grass vegetation regardless of sampling position and depth (Table 3). The same trend is observed for the minimum and maximum D-excess values of soil water. D-excess values in soil water were smaller and presented a lower temporal variability than those in precipitation as depicted by the low standard deviation of the isotopic values of soil water (Table 3).

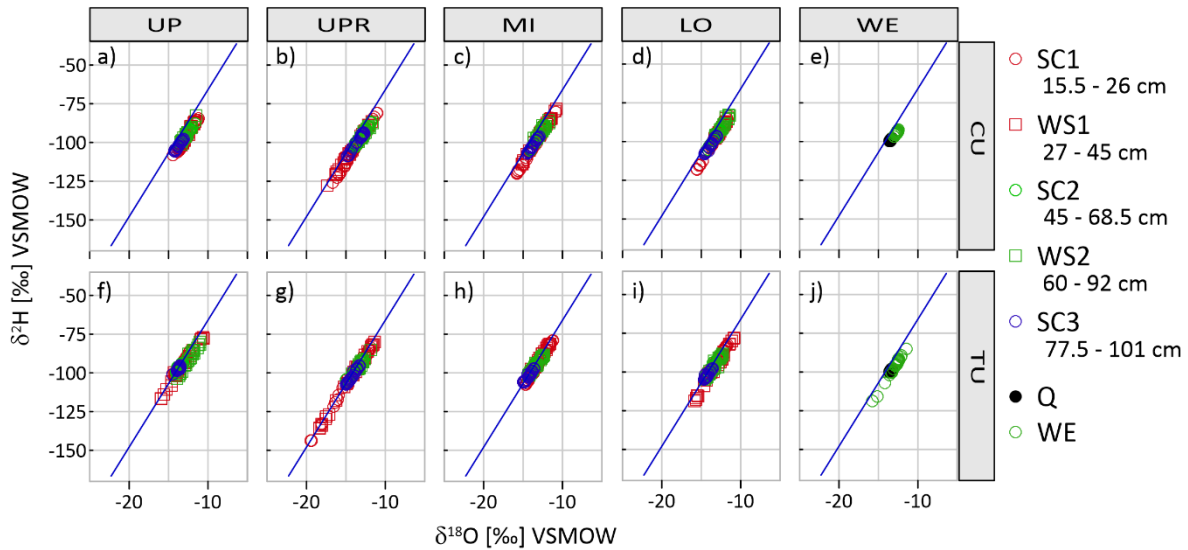


Figure 3  $\delta^{18}\text{O}$ - $\delta^2\text{H}$  relation in soil water collected using suction cups (SC) and wick samplers (WS) at the upper (UP), upper replica (UPR), middle (MI), and lower (LO) parts of the cushion plant (CP) and tussock grass (TU) experimental hillslopes, the wetlands (WE) at the bottom of each hillslope, and discharge at the catchment outlet (Q). Samples were collected biweekly during the period March 2019-March 2020. Sampling depths for each soil water sampler are shown below the sampler code.

The spatio-temporal dynamic of soil water isotopic composition is shown in Fig 4. The attenuation of the isotopic composition of soil water tended to increase as the sampling depth increased. However, different soil water mixing dynamics are observed when the isotopic composition of soils and precipitation are compared. For instance, the isotopic composition of soil water showed isotopic dynamics similar to that of precipitation at all sampling positions in CU\_SC1 and TU\_WS1 (Fig. 4a, Fig. 4d). That is, the depleted isotopic composition of rainfall during the first rainy period (March to June 2019) caused a depletion in the isotopic composition of soil water a few biweeks later. On the contrary, some sampling sites at shallow depths did not respond to the isotopic composition of precipitation (Fig. 4b). Enriched isotopic values were found at all positions, except at UPR, in the TU\_SC1 samplers during the end of the first rainy season (Fig. 4b) when depleted isotopic values were observed in precipitation. The isotopic composition in TU\_WS2 at the UP position showed a similar trend of isotopic enrichment during the more isotopically depleted precipitation period during the first rainy season (Fig. 4h). Soil water at lower depths (SC2, WS2, and SC3) generally had more attenuated signals compared to precipitation and soil water at shallower soil layers (Fig. 4e-j).

Table 3. Summary statistics of the isotopic composition ( $\delta^{18}\text{O}$  and D-excess= $\delta^2\text{H}-8 \delta^{18}\text{O}$ ) and inverse transit time proxies (ITTPs) in soil water collected using suction cups (SC) and wick samplers (WS) at the upper (UP), upper replica (UPR), middle (MI), and lower (LO) parts of the cushion plant (CP) and tussock grass (TU) experimental hillslopes, wetlands (WE) at the bottom of the cushion plant (CP) and tussock grass (TU) experimental hillslopes, discharge at the catchment outlet (Q), and precipitation (P) during the period March 2019-March 2020. Sampling depths for each soil water sampler are shown in Table 2. n=number of samples.

Sampler	n	$\delta^{18}\text{O}(\text{‰})$				D excess (‰)				ITTPs	
		max	min	mean	sd*	max	min	mean	sd*		
TU UPR	SC1	27	-11.9	-19.5	-14.5	2.3	13.9	9.9	11.6	1.0	0.49
	WS1	26	-11.3	-18.3	-14.6	2.3	14.1	10.0	11.4	1.0	0.49
	SC2	25	-12.7	-14.9	-13.8	0.7	15.3	10.5	11.8	0.9	0.15
	WS2	21	-11.8	-14.2	-13.1	0.4	13.0	9.1	10.6	1.1	0.09
	SC3	26	-13.3	-15.0	-14.3	0.6	13.8	10.6	11.6	0.8	0.12
TU UP	SC1	27	-11.8	-14.5	-13.1	0.6	15.5	9.4	12.1	1.0	0.12
	WS1	25	-10.6	-16.0	-13.4	1.8	14.7	7.0	10.1	1.6	0.37
	SC2	26	-13.2	-14.0	-13.6	0.3	14.8	11.2	12.2	0.7	0.06
	WS2	25	-11.0	-14.0	-12.3	0.8	12.1	6.6	8.1	1.2	0.17
	SC3	26	-13.5	-14.5	-13.7	0.2	15.1	11.1	12.5	0.8	0.04
TU MI	SC1	27	-11.2	-14.7	-13.1	1.1	13.4	9.0	10.6	1.0	0.23
	WS1	27	-11.6	-14.0	-13.0	0.7	14.7	10.7	12.0	0.8	0.15
	SC2	22	-12.4	-14.2	-13.0	0.6	14.7	10.6	11.7	0.9	0.13
	WS2	25	-12.3	-14.3	-13.3	0.7	14.0	10.1	11.7	1.0	0.15
	SC3	25	-13.6	-15.0	-14.3	0.4	14.7	11.3	12.2	0.9	0.09
TU LO	SC1	26	-11.7	-14.2	-12.8	0.7	13.7	10.4	11.4	0.6	0.15
	WS1	22	-10.9	-15.8	-13.2	1.7	10.3	6.7	8.4	1.0	0.35
	SC2	27	-12.6	-14.5	-13.4	0.6	14.4	9.8	11.2	0.8	0.13
	WS2	23	-12.3	-14.5	-13.4	0.8	13.9	6.2	10.4	1.3	0.16
	SC3	25	-13.6	-14.6	-14.2	0.3	14.3	10.9	11.7	0.7	0.07
CU UPR	SC1	25	-11.0	-16.7	-14.0	1.6	8.4	5.8	7.1	0.8	0.33
	WS1	22	-11.7	-17.4	-14.6	1.6	11.1	7.2	9.3	0.9	0.33
	SC2	27	-11.8	-14.0	-13.1	0.7	9.8	7.0	8.1	0.7	0.15
	WS2	17	-11.6	-13.4	-12.7	0.5	8.9	5.2	7.2	0.9	0.10
	SC3	25	-12.7	-14.8	-13.4	0.7	9.9	7.3	8.6	0.6	0.14
CU UP	SC1	26	-11.2	-14.4	-13.0	0.8	7.0	3.4	4.9	0.9	0.18
	WS1	16	-11.6	-13.3	-12.3	0.6	8.1	4.1	6.0	1.1	0.13
	SC2	23	-11.6	-13.1	-12.5	0.4	6.9	5.0	5.9	0.4	0.08
	WS2	14	-11.5	-13.5	-12.8	0.5	9.6	5.4	7.2	1.0	0.11
	SC3	24	-13.1	-14.3	-13.7	0.4	8.6	7.0	7.6	0.4	0.08
CU MI	SC1	26	-10.9	-15.8	-13.8	1.5	8.5	5.2	6.7	0.8	0.31
	WS1	23	-10.8	-15.2	-12.8	1.4	9.2	6.8	7.8	0.7	0.29
	SC2	26	-12.1	-14.1	-12.8	0.6	8.3	6.7	7.4	0.5	0.13
	WS2	20	-11.7	-13.6	-12.7	0.5	11.8	6.1	8.7	1.3	0.11
	SC3	25	-13.0	-14.5	-13.8	0.5	8.8	7.4	8.0	0.4	0.10
CU LO	SC1	23	-11.4	-15.6	-13.7	1.3	8.6	6.0	7.2	0.9	0.27
	WS1	21	-11.8	-13.3	-12.6	0.5	10.1	7.0	7.7	0.7	0.11
	SC2	24	-12.5	-14.4	-13.2	0.6	8.9	7.2	8.0	0.5	0.12
	WS2	20	-11.4	-13.2	-12.4	0.6	11.0	7.0	8.3	0.9	0.13
	SC3	26	-13.0	-14.6	-13.7	0.5	9.0	6.4	8.1	0.5	0.11
TU WE	27	-11.4	-15.8	-12.9	0.9	7.8	5.4	6.9	0.6	0.19	
CU WE	27	-12.5	-13.0	-12.7	0.2	7.8	6.1	7.1	0.4	0.03	
Q	27	-13.3	-13.6	-13.5	0.1	9.0	8.3	8.6	0.2	0.01	
P	27	-6.4	-22.3	-12.4	4.8	16.8	8.7	13.6	2.3	-	

ITTPs is the ratio between  $\delta^{18}\text{O}$  standard deviation in an outflow to the standard deviation of  $\delta^{18}\text{O}$  in precipitation.

\*sd: standard deviation

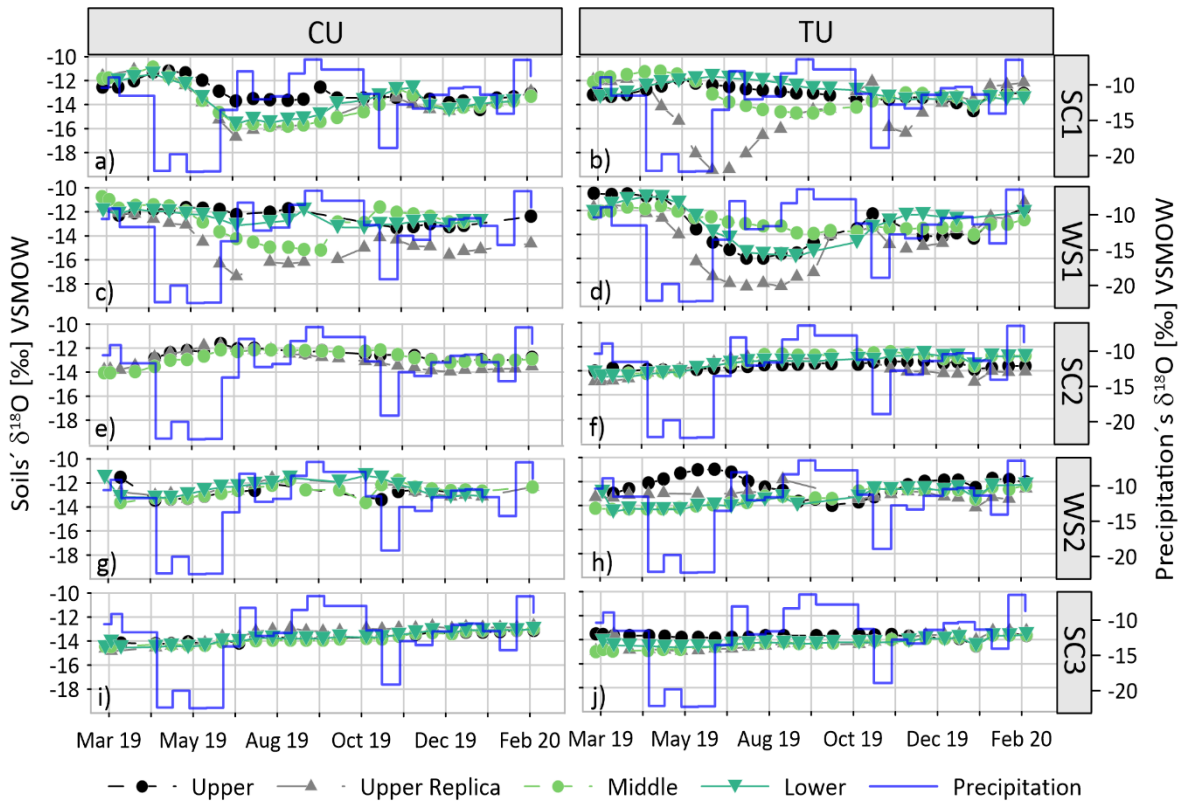


Figure 4. Spatio-temporal variation of the biweekly isotopic composition of precipitation (blue lines) and soil water collected using suction cups (SC) and wick samplers (WS) at the upper (UP), upper replica (UPR), middle (MI), and lower (LO) parts of the cushion plant (CP) and tussock grass (TU) experimental hillslopes during the period March 2019-March 2020. Sampling depth for each soil water sampler is shown in Table 2. Blue line represents precipitation isotopic composition, and it is scaled according to y axis values presented at the right of the figure.

The time series of the isotopic composition of wetlands and discharge are presented in Fig. 5. CU\_WE and Q (discharge) presented attenuated isotopic compositions with almost negligible variation throughout the whole study period (Table 3, Fig. 5a and Fig. 5c). Even though TU\_WE presented an attenuated signal during the dry periods when the isotopic composition of precipitation was enriched, its isotopic signal decreased during wetter periods when the isotopic composition of precipitation decreased (Fig. 5b).

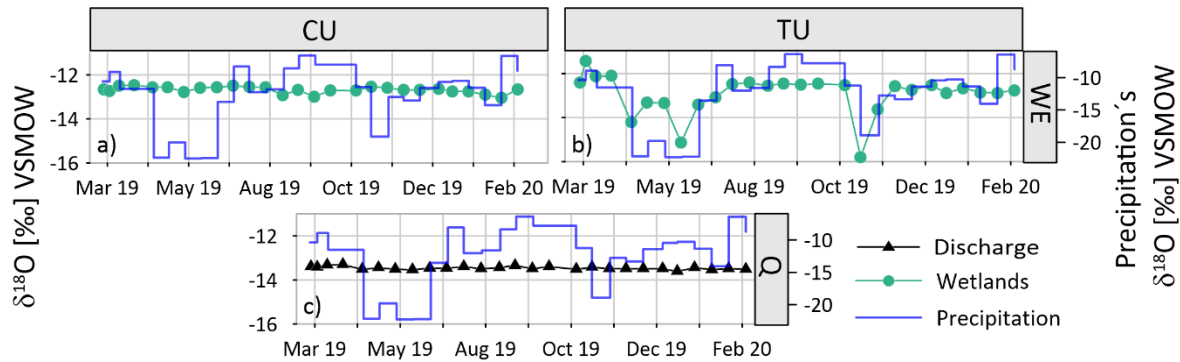


Figure 5. Spatio-temporal variation of the biweekly isotopic composition of precipitation (blue lines), wetlands (WE) at the bottom of the cushion plant (CU) and tussock grass (TU) experimental hillslopes, and discharge at the catchment outlet (Q) during the period March 2019-March 2020. Blue line represents precipitation isotopic composition, and it is scaled according to y axis values presented at the right of the figure.

### 3.3 Mixing processes along the catchment

As a proxy for mixing processes within the study catchment, we used the ITTP metric (Fig. 6 and Table 3). Discharge at the catchment outlet presented the lowest ITTP value (0.01) among all sampling sites (Table 3). Wetlands had ITTP values of 0.03 and 0.19 for the CU and TU hillslopes respectively. The soils' ITTPs presented in Fig. 6 show that they generally decrease with depth regardless of the topographic position. The shallower collectors SC1 and WS1 showed the largest ITTPs along both experimental hillslopes. However, lower values than expected for shallow collectors were found (circles in Fig. 6).

Within the cushion plants experimental hillslope, the UP\_WS1 and LO\_WS1 shallow collectors had ITTPs of 0.13 and 0.11, respectively. These values are lower than ITTPs found in deeper soil layers such as UPR\_SC3 (0.14). For deeper soil collectors (SC2, WS2, SC3) the ITTP values were small and their variation with depth is not clear, with values usually lower than 0.15. The UP\_SC3 showed the lowest ITTP of all along this experimental hillslope (0.08).

Regarding the tussock grass experimental hillslope, three shallow soil water sampling sites showed ITTPs lower than 0.16 (UP\_SC1, LO\_SC1, and MI\_WS1). Similar to the cushion plant hillslope, within the tussock grass hillslope at sampling depths below SC2 the ITTPs were small, generally lower than 0.2. An upper position sampling site showed the lowest ITTP, specifically, UP\_SC3 (0.04). The second lower ITTP is also in the upper position, namely, the UP\_SC2 with a ITTP of 0.06. As can be noticed, shallow soil water samplers showed the biggest ITTPs but samplers from SC2 and deeper did not show a clear difference regarding ITTPs in the two experimental hillslopes.

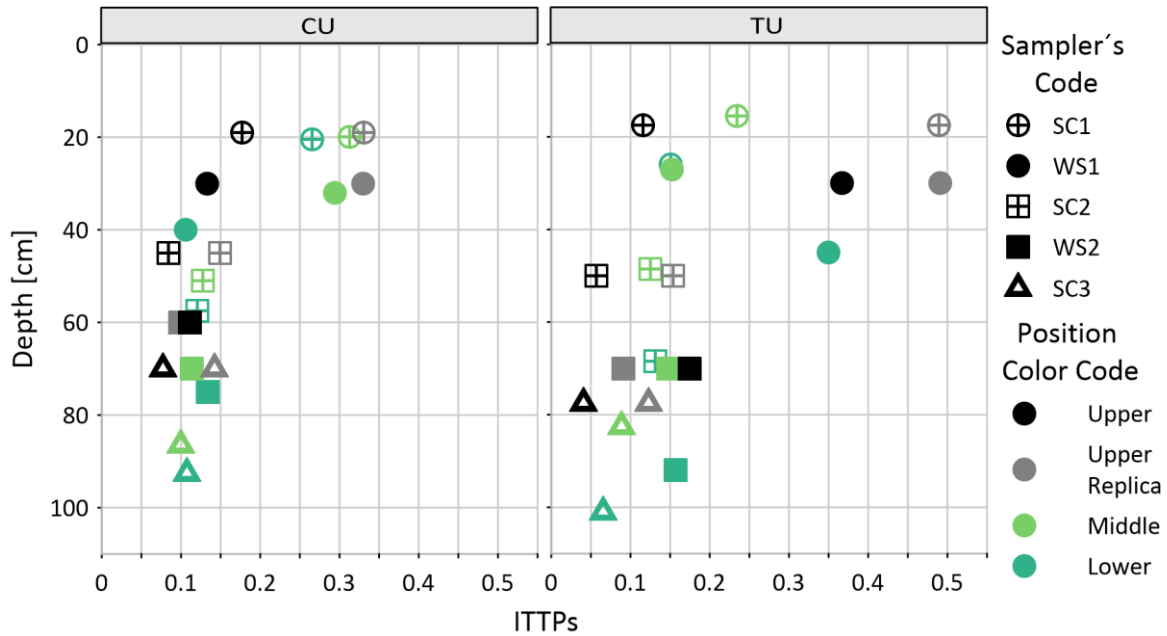


Figure 6. Inverse Transit Time Proxies (ITTPs) of soil water collected using suction cups (SC) and wick samplers (WS) at the upper (UP), upper replica (UPR), middle (MI), and lower (LO) parts of the cushion plant (CU) and tussock grass (TU) experimental hillslopes versus sampling depth. Sampling depths for each soil water sampler are shown in Table 2.

## 4. Discussion

### 4.1 Isotopic spatio-temporal patterns in precipitation

The similar slope of the LMWL (8.2) and GMWL (8; Dansgaard, 1964; Rozanski et al., 1993) indicates that condensation prior precipitation occurs under isotopic equilibrium conditions (Clark & Fritz, 1997; Kendall & McDonnell, 1998). These conditions are likely to occur in the paramos given their relatively homogenous meteorological conditions with low temporal seasonality throughout the year (Celleri et al., 2007). The higher D-excess of the LMWL (16.15 ‰) in relation to the GMWL (10‰) shows that local precipitation is likely influenced by recycled water vapor (Esquivel-Hernández et al., 2019). This effect is likely to occur in the Amazon forest (Gat & Matsui, 1991; Salati et al., 1979) where water is recycled before reaching the Andean highlands of JTU-01. The temporal dynamic of the isotopic composition of precipitation during the study period showed the so-called seasonal and amount effects (Rozanski et al., 1993). That is, the isotopic composition of precipitation was usually enriched during the dryer periods with low precipitation amounts, whereas it was depleted during the rainy periods with high precipitation inputs. Our results are in line with those reported at montane sites in the south Ecuadorian Andes (Mosquera et al., 2012; Mosquera, Céleri, et al., 2016; Windhorst et al., 2013) in which the slopes and intercepts (D-excess) of the LMWLs were close to 8 and larger than 10‰. However, longer and finer temporal resolution precipitation isotopic



records are necessary to carry out a thorough assessment of the origin of the air masses forming local precipitation and the factors influencing its isotopic composition.

#### **4.2 Spatio-temporal patterns in soils, wetlands, and discharge**

D-excess values in soil water in the cushion plant experimental hillslope were lower than those in precipitation (Table 3), indicating that the isotopic composition of  $\delta^2\text{H}$  changed at a faster rate than  $\delta^{18}\text{O}$  in the soil (Leibundgut et al., 2009). From a hydrological point of view, these observations might indicate that soils under cushion plant vegetation are more affected by evaporation than those under tussock grass vegetation since the latter presented D-excess values similar to precipitation (Table 3). This difference could be explained by the protective effect caused by the long needles of tussock grass vegetation, producing a shadow effect that prevents water evaporation to affect shallow soil layers in comparison to the cushion plant vegetation that is directly exposed to solar radiation. It is important to note that D-excess values in soil water did not systematically decrease with depth, which is also consistent with soil water evaporation from the topsoil. By installing soil water collectors in the topsoil, this effect could be assessed in future studies. Discharge and water stored in wetlands also presented lower D-excess values than precipitation (Table 3), indicating that their isotopic signals were also affected by evaporation. Nevertheless, the fact that the isotopic composition of most surface (i.e., discharge) and subsurface (i.e., soil water and wetlands) water samples lied very close to the LMWL (Fig. 3) indicates that the effect of fractionation by evaporation is overall small as has been reported for other paramo sites in south Ecuador (Mosquera et al., 2020; Mosquera, Célleri, et al., 2016). This is likely related to the high infiltration and saturated hydraulic conductivity of the soils (Ochoa-Tocachi et al., 2016; Páez-Bimos et al., 2020).

The temporal dynamic of the isotopic composition of soil water did not show clear differences between the experimental hillslopes. In general, soil water isotopic signals were strongly attenuated with respect to the signal of precipitation, with only a few shallow soil layers resembling the temporal dynamic of the latter (Fig. 4). The isotopic signals were very similar at all sampling sites for most sampling depths, which might point to similar soil hydrological conditions. The observations are in line with those recently reported by Mosquera et al., (2020) for volcanic soils in the paramo of south Ecuador. However, some unexpected effects were observed such as at TU\_UP\_WS2 (Fig. 4h), whose isotopic composition increased while the isotopic composition of rainfall decreased. Since this effect was not found at another sampling site/depth, it could be attributed to local pedological conditions uphill of the soil water sampler (Kirchner, 2016). The diversity of “waveforms”, especially at





shallow sampling depths, show the complexity of water flow paths along the experimental hillslopes. These observations suggest that subsurface flow dynamics in paramo catchments may be different even at small spatial scales as found in other ecosystems (Kim & Jung, 2014; Kirchner, 2016; McDonnell et al., 1991).

The wetlands located below the cushion plant and tussock grass experimental hillslopes presented different isotopic dynamics. The reaction of the tussock grass wetland to depleted precipitation isotopic signal during rainy periods may be due to its location. It situates immediately after the experimental hillslope and so during rainy periods, part of the tussock grass shallow soils may be hydrological active and feed the wetland (Eguchi & Hasegawa, 2008; Hasegawa & Sakayori, 2000; McGuire & McDonnell, 2010; Mosquera, Céleri, et al., 2016). During the less rainy seasons, it appears that the shallow layers of the tussock grass hillslope are not hydrologically active, and that the wetland is hydrologically connected to deeper soil layers presenting more attenuated isotopic signals. Regarding the cushion plant wetland, the strongly attenuated and stable isotopic signal throughout the whole study period probably results due to its location in the middle of the wetland, enhancing water mixing mechanisms (Minaya et al., 2016; Mosquera et al., 2015).

The damping of the isotopic composition that is observed in the river water could be indicative for a mixing of deep subsurface water (Asano et al., 2002). The sole use of water stable isotopes cannot help to unravel the depth or location of this reservoir, and more research is needed to unravel the water storage capacity and transit time of the system (McGuire & McDonnell, 2006).

#### **4.3 Mixing processes along the catchment**

Soil water at shallow depths slightly resembled the isotopic composition of precipitation and had small differences among sampling sites (Fig. 4a-4d), suggesting a low influence of precipitation in mixing with water stored in soils (Mosquera et al., 2020). At lower depths, soil water isotopic composition showed strong damping and little variation with depth regardless of the sampling position in line with the high-water retention capacity of volcanic soils in the paramo (Páez-Bimos et al., 2020). The strong mixing capacity of soil water in deeper soil layers is supported by similar ITTPs (Fig. 6). These findings show the effect of vertical flow paths on soil water percolation. These findings are similar to those reported by Asano et al., 2002; Mosquera et al., 2020; Muñoz-Villers & McDonnell, 2012, including sites dominated by volcanic soils.

Even though wetlands in the southern Ecuadorian paramos do not present isotopic signals as damped as in our study area (Lazo et al., 2019), our results indicate that



Andean Paramo wetlands play a major role in catchment water storage in which water mixes prior to leaving the hydrological system at the catchment outlet (Mosquera et al., 2015) or that they may be an inactive hydrological reservoir where water is stored for longer periods of time. The difference in average values of the isotopic composition of wetlands and discharge ( $0.7 \text{ ‰ } \delta^{18}\text{O}$ ) suggests that although the temporal variability of their isotopic composition is almost negligible (except for the tussock grass wetland during the driest periods), they are recharged by different sources and/or during different periods (Correa et al., 2017; Kirchner, 2003). That, since the so-called altitudinal effect is not likely to cause this difference in isotopic composition given that the altitudinal difference in JTU\_01 between the upper and lower part of the tussock grass hillslope is only 59 m and an isotopic lapse rate of  $-0.3 \text{ ‰}$  in  $\delta^{18}\text{O}$  per 100 m elevation increase has been reported in a paramo ecosystem in south Ecuador (Mosquera, Célleri, et al., 2016). Therefore, long-term data is necessary to further investigate this issue.

Having the historical input signal would have helped to determine how old is the water stored in different catchment compartments (i.e., soil water, wetlands, and discharge). However, our results can help to develop a preliminary but valuable conceptual model of catchment hydrology (Hrachowitz et al., 2016), where discharge is fed by a hydrological reservoir presenting complete mixing conditions (Mosquera, Segura, et al., 2016). The depth of this reservoir contributing to discharge is not yet clear, but it may be composed of water from deeper soil layers (a few to tens of meters deep) and/or fractures in the shallow bedrock. Nevertheless, the presented isotopic dataset provided valuable insights into catchment hydrology in the northern Andes of Ecuador complementing tracer studies performed at higher temporal resolution (Minaya et al., 2016) but without long-term data. This information can be used by local stakeholders, water managers, and decision-makers (e.g., FONAG and EPMAPS). For example, it is observed that all the water produced in this catchment, even during stormflow events (Silva Palmay & Ortiz Moya, 2020), comes from a deep water reservoir standing out the role of soils and wetlands as water regulators in these ecosystems (Lazo et al., 2019; Mosquera et al., 2020; Mosquera, Célleri, et al., 2016). Besides, our data can be coupled with hydrological models, where calibration should consider that most of the water is produced in reservoirs with a complete mixing, even during periods of high rainfall intensity. Finally, the isotopic information could be used in combination with geochemical data and high frequency tracers data (Correa et al., 2018; Minaya et al., 2016) to further improve the process-based understanding of the hydrology of the different Andean catchments in northern Ecuador.



## 5. Conclusions

Catchment hydrology of a small experimental paramo catchment was investigated using a biweekly dataset set of the stable isotopic composition of precipitation, soil water, wetlands, and discharge. Condensation at the study site seems to occur under equilibrium conditions as evidenced by the similar slope of the LMWL (8.2) compared to that of the GMWL (8). The larger D-excess of the former (16.2‰) as compared to the latter (10‰) suggests that local precipitation might be influenced by recycled moisture from the Amazon Basin. Soil water (at shallow soil layers), wetlands, and discharge are little affected by evaporation effects, although future investigation should assess this effect in the shallow layer of the soil where evaporation could be expected to be more influential. Isotopic attenuation of soil water was homogeneous at all sampling positions along both experimental hillslopes, increasing with depth regardless of the ground vegetation cover. Wetlands and discharge showed an almost invariant isotopic composition during the study period showing the importance of well-mixed reservoirs in the hydrology of the system. Although ITTPs showed a decreasing trend with depth, a clear pattern was not observed, highlighting the complexity of the hydrology of the study area. Even though longer isotopic datasets combined with complementary hydrometric and geochemical information are needed to improve the understanding of catchment hydrology in our study site, these findings are useful for water managers working in the region as it improves our general understanding of the complex hydrological behavior of paramo catchments in northern Ecuador. These findings can also serve as a basis to test hypothesis of discharge generation using complementary geochemical information and mathematical models.



## 6. Appendix A

### Summary of precipitation isotopic composition

Campaign	Date	$\delta^{18}\text{O}$ (‰)	$\delta^2\text{H}$ (‰)	D_excess (‰)	Cumulative Precipitation (mm)
1	12/3/2019	-10.38	-69.87	13.15	14.4
2	18/3/2019	-8.93	-60.13	11.27	7.1
3	27/3/2019	-11.52	-77.50	14.67	65.9
4	9/4/2019	-16.85	-119.72	15.04	77.5
5	25/4/2019	-22.17	-161.94	15.41	53.3
6	8/5/2019	-19.80	-149.75	8.66	19.6
7	22/5/2019	-22.28	-168.73	9.55	55.3
8	5/6/2019	-22.22	-164.54	13.25	65.5
9	19/6/2019	-13.53	-96.28	11.96	21.8
10	3/7/2019	-8.07	-49.28	15.26	12.9
11	16/7/2019	-12.03	-82.76	13.52	21.9
12	31/7/2019	-11.61	-79.31	13.55	14.4
13	15/8/2019	-8.36	-51.88	15.03	12.9
14	28/8/2019	-6.39	-35.15	15.94	9.3
15	11/9/2019	-7.80	-46.33	16.05	4.9
16	24/9/2019	-9.32	-58.54	16.03	50.5
17	16/10/2019	-11.25	-73.23	16.77	30.4
18	29/10/2019	-18.92	-138.44	12.91	68.5
19	13/11/2019	-12.77	-87.99	14.16	49.6
20	26/11/2019	-13.33	-92.02	14.63	53.2
21	10/12/2019	-11.40	-80.49	10.71	23.7
22	26/12/2019	-10.45	-69.76	13.86	29.7
23	7/1/2020	-10.29	-72.34	9.96	23.4
24	21/1/2020	-11.36	-78.21	12.69	3.3
25	4/2/2020	-14.06	-100.89	11.57	39.5
26	18/2/2020	-6.44	-35.51	15.98	1.0
27	3/3/2020	-8.73	-53.63	16.21	57.8



## 7. References

- Aparecido, L. M. T., Teodoro, G. S., Mosquera, G., Brum, M., de V. Barros, F., Pompeu, P. V., Rodas, M., Lazo, P., Müller, C. S., Mulligan, M., Asbjornsen, H., Moore, G. W., & Oliveira, R. S. (2017). Ecohydrological drivers of Neotropical vegetation in montane ecosystems. *Ecohydrology*, 11(3). <https://doi.org/10.1002/eco.1932>
- Asano, Y., Uchida, T., & Ohte, N. (2002). Residence times and flow paths of water in steep unchannelled catchments, Tanakami, Japan. *Journal of Hydrology*, 261(1–4), 173–192. [https://doi.org/10.1016/S0022-1694\(02\)00005-7](https://doi.org/10.1016/S0022-1694(02)00005-7)
- Brooks, J. R., Wigington, P. J., Phillips, D. L., Comeleo, R., & Coulombe, R. (2012). Willamette River Basin surface water isoscape ( $\delta^{18}\text{O}$  and  $\delta^2\text{H}$ ): temporal changes of source water within the river. *Ecosphere*, 3(5), art39. <https://doi.org/10.1890/es11-00338.1>
- Buytaert, W., & Bièvre, B. De. (2012). Water for cities: The impact of climate change and demographic growth in the tropical Andes. *Water Resources Research*, 48(8), 1–13. <https://doi.org/10.1029/2011WR011755>
- Buytaert, W., Wyseure, G., Bièvre, B. De, & Deckers, J. (2005). The effect of land-use changes on the hydrological behaviour of Histic Andosols in south Ecuador. *Hydrological Processes*, 19(20), 3985–3997. <https://doi.org/10.1002/hyp.5867>
- Calispa, M., van Ypersele, R., Pereira, B., & Páez-Bimos, S. (2021). *Soil organic carbon stocks under different páramo vegetation covers in Ecuador's northern Andes*. May, 21–22.
- Céleri, R., & Feyen, J. (2009). The Hydrology of Tropical Andean Ecosystems: Importance, Knowledge Status, and Perspectives. *Mountain Research and Development*, 29(4), 350–355. <https://doi.org/10.1659/mrd.00007>
- Celleri, R., Willems, P., Buytaert, W., & Feyen, J. (2007). Space–time rainfall variability in the Paute Basin, Ecuadorian. *HYDROLOGICAL PROCESSES*, 24(1), 318–326. <https://doi.org/10.1002/hyp.6575>
- Clark, I., & Fritz, P. (1997). Environmental Isotopes in Hydrogeology. In *Water Encyclopedia*. <https://doi.org/10.1002/047147844X.gw211>
- Correa, A., Breuer, L., Crespo, P., Céleri, R., Feyen, J., Birkel, C., Silva, C., & Windhorst, D. (2018). Spatially distributed hydro-chemical data with temporally high-resolution is needed to adequately assess the hydrological functioning of headwater catchments. *Science of The Total Environment*, 651, 1613–1626. <https://doi.org/10.1016/j.scitotenv.2018.09.189>
- Correa, A., Windhorst, D., Tetzlaff, D., Crespo, P., Céleri, R., Feyen, J., & Breuer,



- L. (2017). Temporal dynamics in dominant runoff sources and flow paths in the Andean Páramo. *Water Resources Research*, 53(7), 5998–6017. <https://doi.org/10.1002/2016WR020187>
- Craig, H. (1961). Standard for Reporting Concentrations of Deuterium and Oxygen-18 in Natural Waters. *Science*, 133(1958), 18–19.
- Crespo, P. J., Feyen, J., Buytaert, W., Bücken, A., Breuer, L., Frede, H. G., & Ramírez, M. (2011). Identifying controls of the rainfall-runoff response of small catchments in the tropical Andes (Ecuador). *Journal of Hydrology*, 407(1–4), 164–174. <https://doi.org/10.1016/j.jhydrol.2011.07.021>
- Dansgaard, W. (1964). Stable isotopes in precipitation. *Tellus*, 16(4), 436–468. <https://doi.org/10.3402/tellusa.v16i4.8993>
- Eguchi, S., & Hasegawa, S. (2008). Determination and Characterization of Preferential Water Flow in Unsaturated Subsoil of Andisol. *Soil Science Society of America Journal*, 72(2), 320–330. <https://doi.org/10.2136/sssaj2007.0042>
- EPMAPS, & FONAG. (2018). *Actualización del plan de manejo del área de conservación hídrica Antisana*. 99.
- Esquivel-Hernández, G., Mosquera, G. M., Sánchez-Murillo, R., Quesada-Román, A., Birkel, C., Crespo, P., Céleri, R., Windhorst, D., Breuer, L., & Boll, J. (2019). Moisture transport and seasonal variations in the stable isotopic composition of rainfall in Central American and Andean Páramo during El Niño conditions (2015-2016). *Hydrological Processes*.
- Falkenmark, M., & Folke, C. (2002). The ethics of socio-ecohydrological catchment management: Towards hydrosolidarity. *Hydrology and Earth System Sciences*, 6(1), 1–9. <https://doi.org/10.5194/hess-6-1-2002>
- FAO. (2015). *World reference base for soil resources 2014 International soil classification system*.
- Gat, J. R., & Matsui, E. (1991). Atmospheric water balance in the Amazon basin: An isotopic evapotranspiration model. *Journal of Geophysical Research*, 96(D7), 13179. <https://doi.org/10.1029/91JD00054>
- Hall, M. L., Mothes, P. A., Samaniego, P., Militzer, A., Beate, B., Ramón, P., & Robin, C. (2017). Antisana volcano: A representative andesitic volcano of the eastern cordillera of Ecuador: Petrography, chemistry, tephra and glacial stratigraphy. *Journal of South American Earth Sciences*, 73, 50–64. <https://doi.org/10.1016/j.jsames.2016.11.005>
- Hasegawa, S., & Sakayori, T. (2000). Monitoring of matrix flow and bypass flow through the subsoil in a volcanic ash soil. *Soil Science and Plant Nutrition*, 46(3), 661–671. <https://doi.org/10.1080/00380768.2000.10409131>



- Hrachowitz, M., Benettin, P., van Breukelen, B. M., Fovet, O., Howden, N. J. K., Ruiz, L., van der Velde, Y., & Wade, A. J. (2016). Transit times-the link between hydrology and water quality at the catchment scale. *Wiley Interdisciplinary Reviews: Water*, 3(5), 629–657. <https://doi.org/10.1002/wat2.1155>
- Inamdar, S., Dhillon, G., Singh, S., Dutta, S., Levia, D., Scott, D., Mitchell, M., Stan, J. Van, & McHale, P. (2013). Temporal variation in end-member chemistry and its influence on runoff mixing patterns in a forested, Piedmont catchment. *Water Resources Research*, 49(4), 1828–1844. <https://doi.org/10.1002/wrcr.20158>
- Jasper, O., Dietrich, W., Dawson, T., & Fung, I. (2015). Dynamic, structured heterogeneity of water isotopes inside hillslopes. *Water Resources Research*, 51, 5974–5997. <https://doi.org/10.1002/2014WR015608>.Received
- Kendall, C., & Coplen, T. B. (2001). *Distribution of oxygen-18 and deuterium in river waters across the United States*. 1393(September 2000), 1363–1393. <https://doi.org/10.1002/hyp.217>
- Kendall, C., & McDonnell, J. J. (1998). *Isotope Tracers in Catchment Hydrology*. 80(23), 1999.
- Kim, S., & Jung, S. (2014). Estimation of mean water transit time on a steep hillslope in South Korea using soil moisture measurements and deuterium excess. *Hydrological Processes*, 28(4), 1844–1857. <https://doi.org/10.1002/hyp.9722>
- Kirchner, J. W. (2003). A double paradox in catchment hydrology and geochemistry. *Hydrological Processes*, 17(4), 871–874. <https://doi.org/10.1002/hyp.5108>
- Kirchner, J. W. (2016). Aggregation in environmental systems-Part 1: Seasonal tracer cycles quantify young water fractions, but not mean transit times, in spatially heterogeneous catchments. *Hydrology and Earth System Sciences*, 20(1), 279–297. <https://doi.org/10.5194/hess-20-279-2016>
- Lazo, P. X., Mosquera, G. M., McDonnell, J. J., & Crespo, P. (2019). The role of vegetation, soils, and precipitation on water storage and hydrological services in Andean Páramo catchments. *Journal of Hydrology*, 572, 805–819. <https://doi.org/10.1016/j.jhydrol.2019.03.050>
- Leibundgut, C., Maloszewski, P., & Külls, C. (2009). *Tracers in Hydrology* (H. Leister & I. Kohn (eds.)). Wiley-Blackwell.
- McDonnell, J. J., Owens, I. F., & Stewart, M. K. (1991). a Case Study of Shallow Flow Paths IN A STEEP ZERO-ORDER BASIN. *Water Resources Bulletin*, 27(4), 679–685.



- McGuire, K. J., & McDonnell, J. J. (2006). A review and evaluation of catchment transit time modeling. *Journal of Hydrology*, 330(3–4), 543–563. <https://doi.org/10.1016/j.jhydrol.2006.04.020>
- McGuire, K. J., & McDonnell, J. J. (2010). Hydrological connectivity of hillslopes and streams: Characteristic time scales and nonlinearities. *Water Resources Research*, 46(10), 1–17. <https://doi.org/10.1029/2010WR009341>
- Minaya, V., Camacho Suarez, V., Wenninger, J., & Mynett, A. (2016). Quantification of runoff generation from a combined glacier and páramo catchment within an Ecological Reserve in the Ecuadorian highlands. *Hydrology and Earth System Sciences Discussions*, November, 1–20. <https://doi.org/10.5194/hess-2016-569>
- Molina, A., Vanacker, V., Corre, M. D., & Veldkamp, E. (2019). Patterns in Soil Chemical Weathering Related to Topographic Gradients and Vegetation Structure in a High Andean Tropical Ecosystem. *Journal of Geophysical Research: Earth Surface*, 124(2), 666–685. <https://doi.org/10.1029/2018JF004856>
- Mook, W. G. (2000). Environmental isotopes in the hydrological cycle, principles and applications. Volume III: Surface water. *International Atomic Energy Agency*, 1(39), 1–291. [http://www.hydrology.nl/images/docs/ihp/Mook\\_VI.pdf](http://www.hydrology.nl/images/docs/ihp/Mook_VI.pdf)
- Mosquera, G. M., Célleri, R., Lazo, P. X., Vaché, K. B., Perakis, S. S., & Crespo, P. (2016). Combined use of isotopic and hydrometric data to conceptualize ecohydrological processes in a high-elevation tropical ecosystem. *Hydrological Processes*, 30(17), 2930–2947. <https://doi.org/10.1002/hyp.10927>
- Mosquera, G. M., Crespo, P., Breuer, L., Feyen, J., & Windhorst, D. (2020). Water transport and tracer mixing in volcanic ash soils at a tropical hillslope: A wet layered sloping sponge. *Hydrological Processes*, 34(9), 2032–2047. <https://doi.org/10.1002/hyp.13733>
- Mosquera, G. M., Lazo, P., Cárdenas, I., & Crespo, P. (2012). Identificación de las principales fuentes de agua que aportan a la generación de escorrentía en zonas Andinas de páramo húmedo: mediante el uso de los isótopos estables deuterio y oxígeno-18. *MASKANA*, 3(2), 87–105. <https://doi.org/10.18537/mskn.03.02.07>
- Mosquera, G. M., Lazo, P., Célleri, R., Wilcox, B., & Crespo, P. (2015). Runoff from tropical alpine grasslands increases with areal extent of wetlands. *Catena*, 125, 120–128. <https://doi.org/10.1016/j.catena.2014.10.010>
- Mosquera, G. M., Segura, C., Vaché, K. B., Windhorst, D., Breuer, L., & Crespo, P. (2016). Insights into the water mean transit time in a high-elevation tropical ecosystem. *Hydrology and Earth System Sciences*, 20(7), 2987–3004. <https://doi.org/10.5194/hess-20-2987-2016>





- Muñoz-Villers, L. E., Geissert, D. R., Holwerda, F., & McDonnell, J. J. (2016). Factors influencing stream baseflow transit times in tropical montane watersheds. *Hydrology and Earth System Sciences*, 20(4), 1621–1635. <https://doi.org/10.5194/hess-20-1621-2016>
- Muñoz-Villers, L. E., & McDonnell, J. J. (2012). Runoff generation in a steep, tropical montane cloud forest catchment on permeable volcanic substrate. *Water Resources Research*, 48(9), 1–17. <https://doi.org/10.1029/2011WR011316>
- Ochoa-Tocachi, B. F., Buytaert, W., Bièvre, B. De, Céleri, R., Crespo, P., Villacís, M., Llerena, C. A., Acosta, L., Villazón, M., Gualpa, M., Gil-Ríos, J., Fuentes, P., Olaya, D., Viñas, P., Rojas, G., & Arias, S. (2016). Impacts of land use on the hydrological response of tropical Andean catchments. *Hydrological Processes*, 30(22), 4074–4089. <https://doi.org/10.1002/hyp.10980>
- Onderet, C. (2018). *Impact des changements de végétation sur les propriétés des sols des páramos équatoriens : étude de cas dans la réserve de l'Antisana*.
- Páez-Bimos, S., Vanacker, V., Villacís, M., Morales, O., & Calispa, M. (2020). Impact of vegetation species on soil pore system and soil hydraulic properties in the high Andes. *EGU General Assembly 2020, EGU2020-62*. <https://doi.org/https://doi.org/10.5194/egusphere-egu2020-6284>
- Pataki, D. E., Boone, C. G., Hogue, T. S., Jenerette, G. D., McFadden, J. P., & Pincetl, S. (2011). Ecohydrology Bearing - Invited Commentary Socio-ecohydrology and the urban water challenge. *Ecohydrology*, 4, 341–347. <https://doi.org/DOI: 10.1002/eco.209>
- Rozanski, K., Araguás-Araguás, L., & Gonfiantini, R. (1993). *Isotopic Patterns in Modern Global Precipitation*. 1–36. <https://doi.org/10.1029/GM078p0001>
- Salati, E., Dall'Olio, A., Matsui, E., & Gat, J. R. (1979). Recycling of water in the Amazon Basin: An isotopic study. *Water Resources Research*, 15(5), 1250–1258. <https://doi.org/10.1029/WR015i005p01250>
- Silva Palmay, L. F., & Ortiz Moya, E. W. (2020). *Caracterización isotópica de un evento de crecida sobre la microcuenca 1 del Río Jatunhuaycu*. <http://www.dspace.uce.edu.ec/handle/25000/20654>
- Singh, G., Kaur, G., Williard, K., Schoonover, J., & Kang, J. (2018). Monitoring of Water and Solute Transport in the Vadose Zone: A Review. *Vadose Zone Journal*, 17(1), 160058. <https://doi.org/10.2136/vzj2016.07.0058>
- Tetzlaff, D., Seibert, J., McGuire, K. J., Laudon, H., Burns, D. A., Dunn, S. M., & Soulsby, C. (2009). How does landscape structure influence catchment transit time across different geomorphic provinces? *Hydrological Processes*, 23(6), 945–953. <https://doi.org/https://doi.org/10.1002/hyp.7240>



Vanacker, V., Villacís, M., Delmelle, P., De la Torre, E., Dendoncker, N., Cisneros, F., Mora, D., Guevara, A., Molina, A., De Bièvre, B., Lloret, P., Osorio, R., Díaz, C., Barrera, F., & Idrovo, D. (2017). *LINKING GLOBAL CHANGE WITH SOIL AND WATER CONSERVATION IN THE HIGH ANDES*.

Windhorst, D., Waltz, T., Timbe, E., Frede, H. G., & Breuer, L. (2013). Impact of elevation and weather patterns on the isotopic composition of precipitation in a tropical montane rainforest. *Hydrology and Earth System Sciences*, *17*(1), 409–419. <https://doi.org/10.5194/hess-17-409-2013>

Wright, C., Kagawa-Viviani, A., Gerlein-Safdi, C., Mosquera, G. M., Poca, M., Tseng, H., & Chun, K. P. (2017). Advancing ecohydrology in the changing tropics: Perspectives from early career scientists. *Ecohydrology*, *11*(3), 1–18. <https://doi.org/10.1002/eco.1918>